P. K. Phan
Department of Agricultural and Biological Engineering, Mississippi State University, Mississippi, MS 39762; Center of Advanced Vehicular System (CAVS), Mississippi State University, Mississippi, MS 39762

A. T. N. Vo
Department of Agricultural and Biological Engineering, Mississippi State University, Mississippi, MS 39762; Center of Advanced Vehicular System (CAVS), Mississippi State University, Mississippi, MS 39762

A. Bakhtiarydavijani
Center of Advanced Vehicular System (CAVS), Mississippi State University, Mississippi, MS 39762

R. Burch
Center of Advanced Vehicular System (CAVS), Mississippi State University, Mississippi, MS 39762; Department of Industrial and Systems Engineering, Mississippi State University, Mississippi, MS 39762

B. Smith
Department of Industrial and Systems Engineering, Mississippi State University, Mississippi, MS 39762

J. E. Ball
Department of Electrical and Computer Engineering, Mississippi State University, Mississippi, MS 39762

H. Chander
Department of Kinesiology, Mississippi State University, Mississippi, MS 39762

A. Knight
Department of Kinesiology, Mississippi State University, Mississippi, MS 39762

R. K. Prabhu[1]
Department of Agricultural and Biological Engineering, Mississippi State University, Mississippi, MS 39762; Center of Advanced Vehicular System (CAVS), Mississippi State University, Mississippi, MS 39762
e-mail: rprabhu@usra.edu

In Silico Finite Element Analysis of the Foot Ankle Complex Biomechanics: A Literature Review

Computational approaches, especially finite element analysis (FEA), have been rapidly growing in both academia and industry during the last few decades. FEA serves as a powerful and efficient approach for simulating real-life experiments, including industrial product development, machine design, and biomedical research, particularly in biomechanics and biomaterials. Accordingly, FEA has been a "go-to" high biofidelic software tool to simulate and quantify the biomechanics of the foot–ankle complex, as well as to predict the risk of foot and ankle injuries, which are one of the most common musculoskeletal injuries among physically active individuals. This paper provides a review of the in silico FEA of the foot–ankle complex. First, a brief history of computational modeling methods and finite element (FE) simulations for foot–ankle models is introduced. Second, a general approach to build an FE foot and ankle model is presented, including a detailed procedure to accurately construct, calibrate, verify, and validate an FE model in its appropriate simulation environment. Third, current applications, as well as future improvements of the foot and ankle FE models, especially in the biomedical field, are discussed. Finally, a conclusion is made on the efficiency and development of FEA as a computational approach in investigating the biomechanics of the foot–ankle complex. Overall, this review integrates insightful information for biomedical engineers, medical professionals, and researchers to conduct more accurate research on the foot–ankle FE models in the future. [DOI: 10.1115/1.4050667]

[1]Corresponding author.
Manuscript received June 4, 2020; final manuscript received January 13, 2021; published online June 16, 2021. Assoc. Editor: Tamara Reid Bush.

Introduction

Foot and ankle injuries have always been one of the most common musculoskeletal injuries among athletes and other physically active individuals. These injuries include ligament sprains, tendon strains, and bone fractures [1,2]. Studies have shown that foot and ankle injuries can happen to anyone at any age and can also be initiated from different avenues such as sports activities, slipping on an uneven surface, or other types of accidents [3–5]. Foot and ankle injuries are especially common among athletes, who are usually exposed to intense training, which includes jumping and landing or changing directions quickly [6], as well as older adults, who experience a loss of bone density and muscular strength due to aging making them more prone to these types of injuries [7]. Additionally, foot and ankle injuries have long recovery times and effort requirements, and they also make the patients more susceptible to future reoccurrence, strongly affecting their quality of life [3]. As a result, advanced biomedical approaches are needed to analyze the biomechanics of the foot and ankle complex, which can also be used as a practical tool to quantify and predict the risk of injuries during daily activities for both athletes and the general population.

More specifically, with the rapid advancement of computational power and programming over the past several years, there has been extensive growth in the use of advanced software to simulate and analyze complex structures such as bone topography or machine engines in both academia and industry [8,9]. Among those programs, finite element analysis (FEA) is considered as one of the most powerful and productive approaches for predicting how a typical product reacts to real-world forces, vibration, heat, fluid flow, and other physical effects [10]. Thus, due to its practical value, FEA is now an established standard procedure in many areas of numerical strength analysis, such as electrical and industrial machine design [11,12], structural mechanics, and especially biomechanics and biomaterials [13]. In mechanical engineering fields, FEA shows whether a product or a material will break, wear out, or work the way it was designed. In product development, FEA is used to predict the behavior of the product during and after its operation for a particular task. Additionally, FEA plays an important role in state-of-the-art biomedical research since it can replicate and analyze experiments that cannot be conducted on human participants due to the negative implications to the participants such as head impacts, car crashes, or bone fractures [14,15]. FEA models save time and cost compared to real-world experiments. For instance, to get an evaluation of a new type of biomaterial for its effectiveness in research, one might need to carry out large amounts of testing in hospitals and laboratories [16]. However, this method is expensive and time-consuming. By utilizing FEA into the material designing and testing procedure, the work needed will drastically decrease, and the time required to complete an experiment will be shortened. Hence, instead of solely perform real experiments, numerical simulations, and mathematical FEA modeling conducted on a numerical simulation would provide more benefits in terms of cost, timing, control, and flexibility [17]. As a result, there has been an increase in the use of finite element (FE) models to investigate the foot and ankle complex, focusing on biomechanics and its ability to evaluate and predict the injury risks for various gait motions during walking, running, and training [18–21]. To our knowledge, there are only a few review articles that discuss the topic of utilizing FE modeling in analyzing human biomechanics. These articles focus on different parts of the human body, such as joints [22,23], bones [24], and especially, foot and ankle complex [25]. However, the developing procedure of these models, as well as the proper validation and verification methods, has not clearly described accentuating their potential applications. Hence, to provide engineers and researchers a brief description and background about FE modeling of the human foot and ankle, the objective of this paper is to give a detailed summary of the different FE computational approaches in the analysis of foot and ankle complex biomechanics as well as its future potential.

One of the first studies focusing on the biomechanics of the foot–ankle complex dates back to 1988 when Rodgers et al. analyzed a symptom-free foot–ankle complex during upright locomotion to quantitatively evaluate movement dysfunction [26]. In this study, both kinematics and kinetics of the foot and ankle were analyzed during walking and running [26]. Specifically, joint angles were collected from clinical data and experiments to summarize the five main phases in a gait cycle (heel strike, foot flat, midstance, heel-rise, and toe-off) [26]. Electromyographic data, as well as pressure distribution and center of pressure from muscles of the lower leg, were also obtained using force plates to develop a mathematical model to compute the muscle and joint reaction force for each gait cycle [26]. Overall, this study successfully illustrated the dynamic biomechanics of the foot and ankle, aiming to aid physicians in the assessment, diagnosis, treatment, prevention, and rehabilitation of foot and ankle injuries.

At the end of the 1990s, one of the first FE models of the foot and ankle was introduced in Tannous et al.'s work to formulate injury tolerances for an axial impact loading event [27]. The model was created based on computerized axial tomography scans of a 50th percentile human ankle, showing 28 different bones, seven ligaments, three retinacula, three layers of plantar soft tissues, and the Achilles tendon. The model, consisting of over 17,000 elements, was likely considered to be one of the most biofidelic foot and ankle models at the time. After the model was generated, it went through two simulations of axial impact loading at two distinct positions, neutral and dorsiflexion, to simulate the event of a car accident. The results obtained from these examinations, ranging from maximum principal stress, maximum shear stress, and maximum principal strain to energy distribution and strain surface contour of various bones, were matched with previous experimental data from the literature [27]. Therefore, despite some minor limitations such as a lack of articular cartilage and overlapping bone structures, this model demonstrated the great potential of an FE approach as a practical tool to evaluate the biomechanics of the human body, especially the foot and ankle complex. As a result, these models and simulations could then be developed to analyze and predict the outcome of different high-risk scenarios, to prevent and reduce injuries potentially.

In recent years, there have been different methods that are applied to modeling the foot and ankle complex, which can be mostly separated into physical models and numerical models [19,28–30]. Specifically, the physical models of the foot and ankle complex can be made from common materials ranging from wood, metal or plastic for various usages (shoemaking, foot mannequins, medical models, etc.), to more advanced, high-end materials such as three-dimensional (3D)-printed alloys or polymers that are utilized in industrial and medical fields, especially for ankle–foot orthoses design [31–33]. At the same time, the swift increase of computational power in recent decades has facilitated the widespread use of complex numerical modeling methods, not only in industry but also in research. Specifically, computational foot and ankle models, generated using the general computational methods such as computer-aided design [18,34] or FE modeling, is a stand-out as a computerized method to evaluate the biomechanics of the foot and ankle complex in medical applications [29,35,36], focusing on gait cycle analysis [18,37,38] as well as predicting and preventing ankle injuries [13,39,40]. However, with the advantages of greater geometric and material biofidelity, lower cost, high accuracy, easy adaptability to complex structures, and the ability to obtain model outputs—such as stress and strain contours, at any location—computational FE models of the foot and ankle complex have been gradually chosen as the suitable and effective approach for foot and ankle complex analysis [35,41]. Thus, to genuinely perceive the potential of FE models of the foot and ankle, it would be better for the users to know how to develop an anatomically correct foot accurately and ankle complex model as well as thoroughly understand the techniques and approaches from a wide range of computational foot and ankle model studies in the recent years. A list of studies that use FE modeling for

analyzing the foot and ankle complex biomechanics is given in Table 1 in the Appendix.

The General Method to Build a Finite Element Foot and Ankle Model

Anatomically Biofidelic Three-Dimensional Reconstruction of the Foot and Ankle Complex. The anatomically biofidelic geometry of the foot and ankle complex can be developed from a set of computed tomography (CT), or magnetic resonance imaging (MRI) scans of an individual [42–44]. The bones, muscles, and connective tissue (tendons and ligaments) are extracted from the procured CT scans based on their Hounsfield unit (HU) (or grayscale value) of each pixel on the images [45]. Subsequently, muscles and soft tissue structures can be extracted more efficiently from MRI scans. Then, a medical 3D image-based engineering software such as SIMPLEWARE SCANIP (Synopsys Inc., Mountain View, CA) or MIMICS (Materialise Mimics® Innovation Suite, Leuven, Belgium) is utilized to manually and semiautomatically segment the different components into a total of 28 parts. The foot and ankle model consists of different sections of bone, which include the tibia, fibula, talus, calcaneus, navicular, cuboid, lateral/intermediate/medial cuneiforms, first to fifth metatarsals, and 14 proximal/middle/distal phalanges [13,30,35]. Additionally, to analyze the basic motions of the foot and ankle complex, ten different groups of muscles, whose functions are closely related to the four typical ankle movements (plantar flexion, dorsiflexion, inversion, and eversion), need to be constructed. These muscles include the tibialis anterior, tibialis posterior, extensor hallucis/digitorum longus, flexor hallucis/digitorum longus, fibularis longus/brevis/tertius, gastrocnemius, and soleus [46]. The inclusion of other muscle groups in the FE model of the foot and ankle complex can be neglected as they do not have a direct impact on the ankle movements [47]. Figure 5 and Table 1 in the Appendix illustrate the constructed muscle groups along with the muscular anatomy and their corresponding functions in foot and ankle movements [48].

Mesh Development. For mesh development, CT or MRI scans from the region of interest can be obtained to use as a background for the FE foot and ankle model. These scans can come in many different file types such as JPEG, PNG, or TIFF; however, Digital Imaging and Communications in Medicine (DICOM) format is preferred in biomedical modeling. The main reason is its ability to automatically organize and scan images into 3D with the corresponding spacing as well as store the biographical data of the particular patient [35]. Due to its characteristics, CT scans are mainly used to archive the bone structures of the model through the use of X-ray, which can effectively pierce through most of the tissue but are not very compatible with bone. Also, MRI scans utilize a strong magnetic field and radiowaves to produce explicit views of muscle and soft tissue [43,44]. As a result, in the case of lacking MRI scans, a recursive smoothing filter could be applied to the CT scans to alleviate the noise and enhance the view on the muscle and tendon groups.

Each pixel of different sections on the scans is identified based on their corresponding HU, also known as grayscale value [45]. HU is defined as a quantitative scale for describing radiodensity, which is a linear transformation from the attenuation coefficient—the measurement of how easily a material can be penetrated by an X-ray beam [45]. To be more specific, every organ inside the human body can fall in a specific range of HU, which helps distinguish pixels of one organ from another. For example, human bone will be in the range of 300–1000 HU, muscle lies between 10 and 40 HU while the liver is around 40–60 HU [49–51]. Additionally, by convention, air will have the HU of −1000 while water gets the HU of 0 [20,45]. Next, to build a background for the FE model, all the scans in 3D are stacked together to create a volume image, which consists of subunits called voxels. Then, by selecting groups of voxels depending on their distinct HU values, a mask of a specific organ enclosing in the chosen HU range is produced. An illustration of this procedure is shown in Fig. 1. As a result, the aforementioned bones, muscles, tendons, and connecting tissue could be accurately built using this approach.

For the next step, a mesh of the FE model can be generated based on the developed masks using common meshing software such as SIMPLEWARE SCANIP), HYPERMESH (Altair HyperWorks, Troy, MI) or ABAQUS FEA (Dassault Systemes Simulia Corp., Johnston, RI). Depending on the shape of each component, the meshes are filled with two-dimensional (2D) elements (such as triangle, quadrilateral) or 3D elements (tetrahedron, hexahedron, pentahedron). To be more specific, when generating a 3D FE model for human bones, hexahedron and tetrahedron are generally utilized to create the mesh. Notably, hexahedral elements are more accurate and efficient when used in a dynamics simulation, while tetrahedral elements allow users to discretize surfaces of complex structures [53]. Due to the complexity of human bone geometry, the choice of assigning sections with element types affects the coarseness of the model (total number of elements) and the computational cost (simulation run time). In general, researchers aim to develop the optimal mesh density where the model accuracy is achieved (conversion of model predictions) with the least number of elements.

Material Properties and Boundary Condition for Model Generation. A final mesh of the foot and ankle model can be converted and exported into simulation software such as ABAQUS or LS-DYNA (Livermore Software Technology Corporation, Livermore, CA) to simulate various ankle movements or gait motions. Notably, before running the simulation, several beams or axial one-dimensional elements, acting as ligaments that connect different bones, are added into the mesh based on ligamentous dissections of the foot and ankle documented in anatomical textbooks, journal papers and illustrations [54–56]. This method is recognized as one of the most efficient approaches to simulate the behavior of ligaments on the foot and ankle complex [34,55].

After generating a mesh, an assortment of properties must be assigned to create the environment for simulation. These properties, depending on different studies and objectives, may comprise

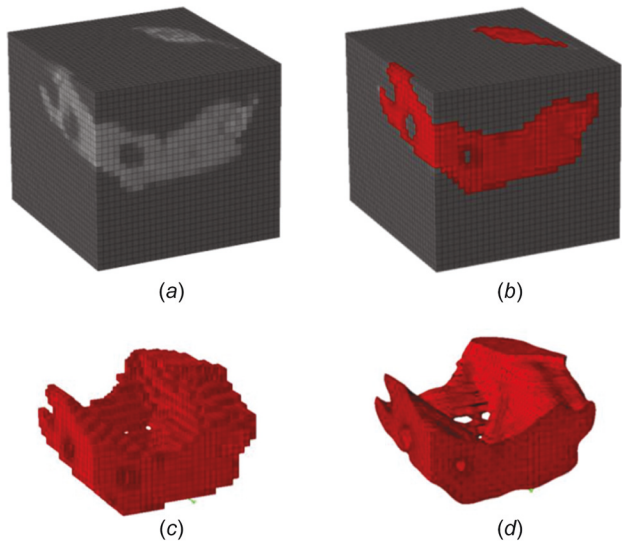

Fig. 1 Illustration of mask creation procedure—Synopsys Proprietary. Used with permission [52]. (*a*) Volume image, which consists of voxels, is generated from CT/MRI scans. (*b*) Sections of interest are selected based on a suitable range of Hounsfield unit. (*c*) Mask of the selected section. (*d*) Smoothen mask prior to being exported to other software.

of material properties, contacts, and constraints, boundary conditions, as well as loads (forces). For the FE model of foot and ankle complex, proper material properties on each particular section of the model can have a direct impact on the model as they can ensure a meaningful response as well as secure the validity of the simulation's results. In order to analyze the movements of the foot, a typical foot and ankle complex model requires correct material properties for bones (both cortical and cancellous), muscle, tendons, ligaments, fascia, soft tissue, and skin. In general, bones are considered to have linear elastic properties, with Young's Modulus ranging from 0.7 GPa to 17.5 GPa for cancellous and cortical bone, respectively [20]. On the other hand, based on the study goals, some features can then be omitted. For instance, when analyzing the performance of ankle prosthesis using the FE model, muscle, tendons, ligaments, and fascia may be omitted to focus on the stress and strain contour on bone surfaces [28,30,36]. When presented, muscle and fascia sections are treated as a linear elastic material (Young's modulus of 0.45 GPa [57] and 0.35 GPa [58], respectively). Soft tissue is then defined using hyperelastic material properties with parameters obtained from experimental data in the literature [59]. Ligaments are consistently modeled as one-dimensional beam elements and can have different lengths and sizes when added into the foot and ankle complex FE model. As a result, their material properties are scaled from a reference segment of a ligament, whose properties are taken from an elastic force–strain relationship considering their cross-sectional areas [20]. To be more specific, if the Young modulus of an anterior talofibular ligament is 1 GPa, a medial plantar cuneonavicular ligament, whose cross-sectional area is 20% of the anterior talofibular, will hold the Young's Modulus of 0.2 GPa [20,60]. Finally, tendon and skin, in the foot model, can also be treated as Ogden hyperelastic material with calibrated parameters from different testing schemes [13,19,61].

Next, after the material properties assignment process, a set of suitable boundary conditions must be implemented in the model. These boundary conditions consist of various constraints, contact properties, and loads, depending on each particular study and intention. Currently, there are two main approaches in analyzing foot and ankle movements: a 3D method and a 2D method for FE models. 3D FE model simulations often use data derived from a force plate—an instrument that measures ground reaction forces generated by a body when standing on or moving across the plates—that simulates the foot movement by serving as the "ground" underneath the participant's footfalls and gathers real-life experimental data. In these FE models, a plate is attached to the sole of the model foot and ankle, acting as the ground supporting the foot. Since the distal tibia and fibula of the foot and ankle model are usually fixed in three directions, various postures and movements can be replicated by turning the plate at a particular angle [30,62]. This results in a twisted or adjusted foot and ankle model that is deformed into a specific posture or movement as assigned by the researchers. For example, by inclining the plate upward on one end (under the toes) while keeping the other half fixed, the dorsiflexion movement could be replicated [20]. Likewise, every simulation has its own set of rotating angles that are selected by the user based on each individual experiment and study.

Conversely, a 2D foot and ankle model can be simulated in a different manner. These 2D models, often taken from the central slide of the corresponding 3D model, take advantage of motion capture technology in simulating the foot and ankle movement [38]. By assigning assorted reference points on the 2D model based on the locations of the markers during the motion capture process, a set of forces acting on these reference points can be computed with respect to each time integration. By utilizing these data, a compatible force field can be applied on each reference point, making them move accordingly to the prerecorded motion and simulating the foot movement in the software environment [38]. This approach requires a fixed thin line under the foot, acting as the ground to fully capture the movement and allow further analysis. Unlike the first approach, this 2D approach does not constrain the foot model in any means and allows it to move freely in space, except the interaction line with the ground [38]. Additionally, the benefits of this approach are the low time and computational cost, being applicable for both gait and foot movement studies or soft tissue analyses. However, due to its own characteristic as a 2D model, the stress distribution or strain surface contour, which usually performs in three dimensions, is hard to capture. In conclusion, depending on the goal and objective of each study, a convenient approach and corresponding boundary condition can be selected from these two methods.

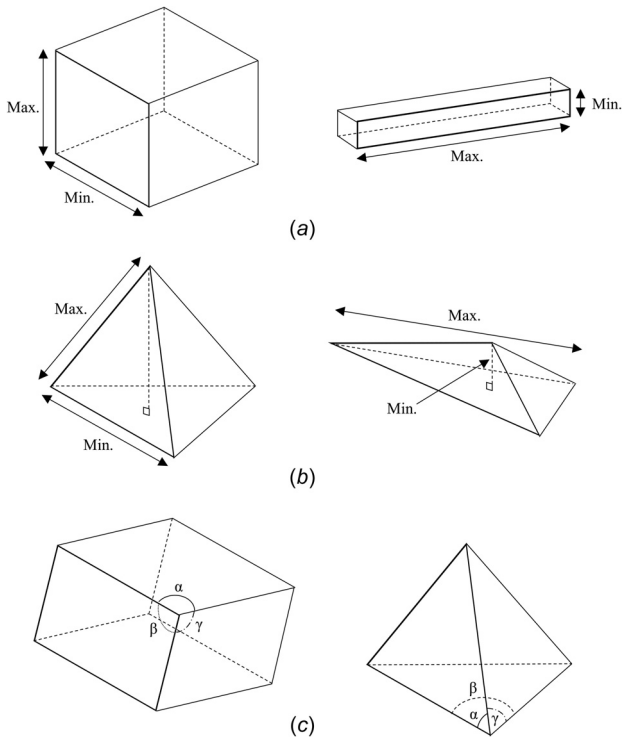

Fig. 2 Illustration of mesh quality metrics, recreated, and modified from Ref. [53]. (*a*) Aspect ratio of 1 versus 14 for hexahedral. (*b*) Aspect ratio of 1 versus 14 for tetrahedral. (*c*) The measured angle at the vertices for each element type (angle idealization).

Mesh Quality Assessment. The accuracy and validity of a simulation are greatly affected by the mesh quality of the model, which consists of three different metrics: aspect ratio (AR), angle idealization, and element Jacobian [53]. In particular, the AR of an element in the mesh is computed by dividing the longest edge to either the shortest edge for the hexagonal element or to the minimum altitude for the tetrahedral elements that can range from one to infinity. Considering the geometrical complexity of human bones with their varying curvature and thickness, the recommended and acceptable AR range that introduces the smallest errors is one to three [63]. Conversely, the mesh quality can also be analyzed through the angle idealization, which demonstrates how the interior angles at each vertex deviate from the ideal angle (90 deg for hexahedral and 60 deg for tetrahedral elements) [53]. The proper values suggested by Burkhart et al. for interior angles are from 30 deg to 120 deg for tetrahedron and less than 160 deg for hexahedron to attain a good result from human bone meshes. Figures 2(*a*) and 2(*b*) below show illustrations of mesh geometry and two aspect ratios for hexahedral and tetrahedral elements. Figure 2(*c*) depicts the angle-based idealized geometry for a hexahedral and tetrahedral mesh.

Finally, the last metric proposed by Knupp et al. involves measuring the volume distortion of each element through the element Jacobians. This value is taken from the determinant of the Jacobian matrix, which defines the mapping from the ideally shaped elements to the current elements generated in the mesh [64]. The three main criteria for the element Jacobians suggested by various studies consist of being positive [64], greater than 0.2 in magnitude [65], and less than 5% of the Jacobian in the model fall below a magnitude of 0.7 [66]. Additionally, the generated mesh can be remeshed by changing the element types and sizes. By reducing the element size near the surfaces of the bone or muscle group while increasing the one inside the structure, a volume mesh of the foot and ankle complex containing hybrid elements with hexahedral elements within each part and tetrahedral elements on each surface can be formed. This method of building the mesh not only could create an anatomically biofidelic model with a smooth and conforming interface between parts and coincident nodes but also could reduce the total number of elements in the model, resulting in shorter simulation run-time in later steps [20].

While FE models and simulations approximately recreate real-life experiments in numerical methods, the fact that they are not real is still undeniable. Hence, a reasonable procedure to verify and validate the results of the simulation is essential. Particularly, energy balance assessment is one of the most favored methods to verify a model that ensures the numerical results of the model follow the basic rule of physics—the conservation of energy [66]. To be more precise, the sum of the potential, kinetic, hourglass, and damping energies must fall within 5% of the total global energy of the system [53]. If hourglass control is used to prevent the model from "hourglassing"—the deformation of hexahedral elements in the absence of the strain—then the hourglass energy should not contribute more than 10% of the total energy [67]. If mass scaling is used, a method that involves adding more mass to the system to reduce simulation times, it must not heavily interfere with the physics of the simulation, especially the kinetic energy.

Finally, the results of the FE simulation need to be validated to guarantee that it adheres to the experimental finding of the same problem. These data can be compared through the use of either validation metrics [65] or statistical methods. In particular, the validation metric (VM), shown in Eq. (1) below, involves the total number of data (N) as well as the simulated and experimental measurements with respect to the simulation time (y, Y, and t, respectively)

$$\mathrm{VM} = 1 - \frac{1}{N}\sum_{n=0}^{N} \tanh\left|\frac{y(t_n) - Y(t_n)}{Y(t_n)}\right| \tag{1}$$

The validation metric yields a value of 1 when the simulated and experimental results are perfectly matched, while it exponentially decreases to 0 as the difference gets larger [53]. However, since VM is sensitive to time between the two datasets as well as the time duration, caution must be exercised when using this method depending on the time signal. Additionally, based on the suggestion of Zhang et al., an error of 10% is considerable between the computational and experimental data [68]. Hence, the authors recommend that the VM of a model should fall within the range of 0.9–1 to be identified as a valid model.

Statistical techniques are another approach to validate the simulation results by comparing them to experimental data from laboratories on either human participants or cadaver studies. These statistical techniques utilize the error assessment and correlation analysis to compare and contrast the mean and standard deviation of the dataset and evaluate the level of agreement between the simulation and experiment. Particularly, percentage errors [69] and root mean squared errors (RMSEs) [70] are used to quantify the differences between some specific values (e.g., peak values of the dataset). In general, the acceptable percentage errors or RMSEs can be identified based on the experimental data as well as the educated guesses of the researchers using prior knowledge about the particular problems [53]. With respect to the experimental data, the recommended RMSE should not be too large (to avoid underfitting) but also not too small (to avoid overfitting). Hence, one cannot claim a universal number as an acceptable RMSE and need to determine the RMSE based on the given information and the accuracy of the current model.

Additionally, correlation analyses are often presented as the Pearson correlation coefficient and provide a measure of the relationship between the experimental and model data [53]. Generally, the Pearson correlation coefficient can take a range of values from $+1$ to -1. A value greater than 0 indicates a positive association; that is, as the value of one variable increases, so does the value of the other variable [71]. In contrast, a value less than 0 indicates a negative association; that is, as the value of one variable increases, the value of the other variable decreases [71]. Hence, in this case, the Pearson coefficient between the experimental and model data should fall between $+0.5$ and $+1$ to archive positive association and ensure the accuracy of the two data sets [53,71]. At this point, depending on the result from the mesh quality assessment, remeshing can be considered for the components that are too asymmetrical or have abnormal metrics to ensure shorter runtime as well as reduce the risk of error during the simulation. Furthermore, the higher the number of elements on the model, the more accurate the results would be. Therefore, a convergence study may be performed to get the optimal results depending on the research's goal [13,15,41,47]. This means repeating the simulation with a higher number of elements until the result starts to converge into a specific value. Eventually, as discussed earlier, this test will ensure that the most reasonable result can be achieved while using the smallest number of elements in the model. All in all, these validation and verification techniques aid users in assuring the confidentiality of the simulation in predicting real-world phenomenon. Figure 3 gives an overview of the data acquisition and preprocessing of the foot and ankle complexes' CT and MRI scans to generate FE mesh. Furthermore, Fig. 3 also shows the FE modeling procedure along with iterative workflow for FE mesh convergence and FE mesh validation with experimental data.

Current Application of Foot and Ankle Finite Element Model

Various studies have focused on the biomechanics of the foot and ankle complex, using both experimental and numerical approaches, in an attempt to identify the cause of ankle injuries as well as predict and lower the potential risk of injuries [20,29,62,72–74]. Since the early 2000s, FEA has been widely used to investigate complex biomechanical relationships in the human body [20,29,30,36,61]. Additionally, FE models have been used to replicate experiments and simulations on diverse subjects of interest (e.g., infants, older adults, people with disabilities) that could not be conducted easily in laboratory settings [75]. Notably, these simulations were applicable in a variety of biomedical topics that range from determining bone fracture thresholds to infant head impacts and collision analyses [75]. There have been a few studies that used FE models, especially in the biomedical and instrumentation fields, to assess the biomechanics of the foot and ankle complex [18,20,38]. Other studies used FEA to evaluate the performance of new medical prosthesis devices [36,76,77], or even predict and mitigate the risk of injury in daily activity for the elderly and athletes [13,78].

The foot and ankle complex FE models are a great software tool to study the human foot and ankle biomechanics. Smolen et al. used a FE model of the foot to simulate the effect of different postures on foot and ankle injuries. Here, Smolen et al. evaluated five different postures to obtain the stress–strain response on the bony surface of the foot as well as predicted the bone fracture threshold and location based on the stress–strain response [20]. Specifically, by fixing the proximal end of the shank and attaching

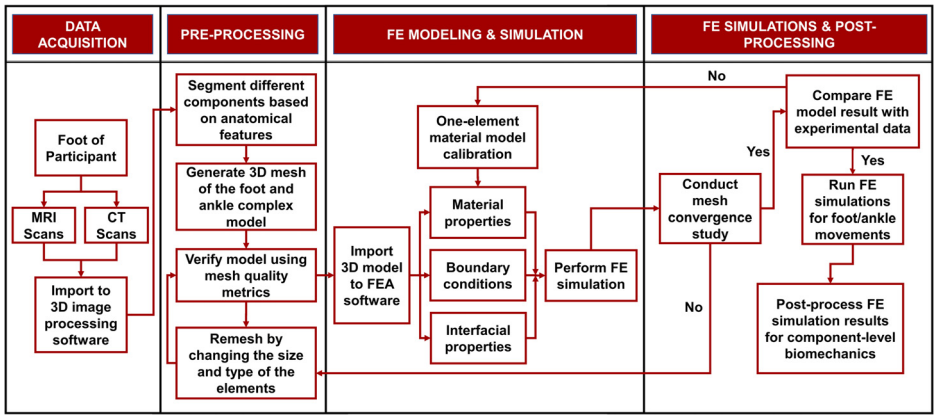

Fig. 3 A work flowchart of the foot and ankle complex FE meshing, modeling, and simulation procedures

a footplate to the plantar surface of the foot, different postures (e.g., neutral, inversion, eversion, dorsiflexion, and plantarflexion) were simulated in this study through rotating the footplate to a particular angle in space. Ultimately, by comparing the data extracted from the strain contour plot to previous literature data as well as experimental data, the bone fracture threshold and location could be validated and predicted [20]. However, some of the limitations associated with this approach included the locations of the strain gauges, the lack of flesh (muscles, tendons, and connecting tissues) in the model and the low number of specimens tested for validation data.

Qian et al. also utilized the FE approach to investigate the dynamic behavior and the internal loading conditions of the human foot and ankle complex during locomotion [38]. By using sagittal plane CT scan images of the participant's foot, a 2D model was created and coupled with force and moment data from experimental gait measurements to simulate one gait cycle of the foot. The FE model was validated by comparing the predicted data of ground reaction force, the center of pressure, and plantar surface pressure to the corresponding experimental data. Researchers from this study propose a simplified approach to investigate the structural dynamics of the human foot musculoskeletal system during normal or even pathological functioning, which formed a foundation for further dynamic foot ankle analysis in the future [38].

Another purpose of using a FE model is to identify the effect of a single component of the structure on the whole foot and ankle complex, as described in Morales-Orcajo et al.'s work [13]. This study analyzed the effect of the tendon forces of the lower limb on the inner foot structure and determined the suitable material properties for the nonlinear behavior of tendons [13]. The FE model used in this study utilized the benefits of both MRI and CT scans to create a model with an accurate and detailed bone, muscle, and tendon structure of the ankle. Then, by performing a force sensitivity analysis of the ankle stabilizer tendons (peroneus, tibialis, and Achilles tendons), Morales-Orcajo et al. successfully replicated the behavior of the foot under compression in two cases (standing and midstance phase) and characterized the tendons as an Ogden first-order hyperelastic material. These results were cross-validated on the vertical displacement of the foot under load as well as plantar pressure distribution [13]. The authors note several limitations in the study that included insufficient bone-to-bone contact, the lack of ligaments on the foot model, and low computer capacity to run the simulation.

Finite element models can also be used as a convenient approach for hypothesis-driven testing for foot and ankle biomechanics analysis. For instance, FE modeling of the foot and ankle complex can be used to investigate the effects of including skin in the simulation [61]. In a study conducted by Ou et al., the material sensitivity of the skin on foot arch deformation was analyzed by simulating upright standing to measure static vertical stiffness, navicular displacement, or plantar aponeurosis strain [61]. By gradually increasing the Young modulus of the skin, foot arch deformation was observed to change when comparing the simulated data to those that included and excluded skin. Moreover, the study also gathered data from cadaveric experiments to validate their results, which is a noteworthy method of verification. Further studies of the foot arch using FE models were carried out by Sun et al., who associated the effects of foot arch height with foot injuries [62]. By establishing three distinct FE foot models with three levels of arch height (low, normal, and high), the stress and strain distribution on foot during upright standing were investigated. These studies uncovered that there was a considerable increase in the stress and strain of the plantar fascia for the high-arched foot as well as a higher stress concentration in the calcaneus, navicular and cuboid in the low-arched foot. Such data provide physicians and researchers valuable information in predicting the injury risk among patients with particular foot arch types [62].

Furthermore, FE models can be a great source of reference to evaluate the performance of implant prosthesis or biomedical devices. In one of the studies from Wang et al., the biomechanical differences of the foot and ankle between the foot with total ankle arthroplasty (TAA) and an intact foot are thoroughly investigated using the FE method [30]. This was done by developing two FE foot models, one for the intact foot and one that contains a three-component ankle prosthesis fixed to the distal tibia. Then, the performance of the prosthesis was investigated through the simulation of the gait stance phase. By comparing the plantar pressure and joint contact pressure between the computational results and the experimental measurements from the cadaveric study, the effect of the prosthesis on the human foot was assessed. To be more specific, the study found that total ankle arthroplasty resulted in a great increase of contact pressure at the medial cuneonavicular joint, hence, making it sustain the highest contact pressure among all joints in the foot [30]. These findings of the biomechanical performance of a prosthesis design would benefit surgeons in preparing surgical protocols to avoid complications and also have a direct impact on future ankle prosthesis design. In the same fashion, Sopher et al. also utilized the FE model to test their implant designs on the tibia in order to reduce the effect of the implant loosening without performing on a real patient [36]. Here, different total ankle replacement (TAR) prostheses were modeled using computer-aided-design geometry and embedded into the tibia and talus of a FE foot and ankle complex. Then, by simulating the physiological loads on the model in various scenarios of optimal positioning as well as malpositioning, the optimal

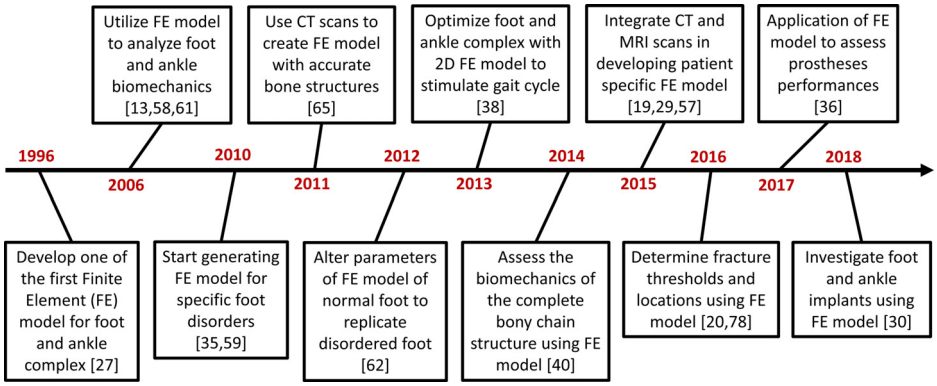

Fig. 4 A timeline evolution of FE modeling of the foot and ankle complex

positions for the TAR prosthesis were determined to alleviate the loosening effect [36]. As a result, the conducted simulation aided researchers and designers in identifying the fixation features and malpositioning cases that can further increase the risk of implant loosening. Figure 4 illustrates a brief history of how FE models of foot and ankle were utilized in various biomechanical applications (see Appendix—Table 2 for more detailed descriptions).

Future Development for Foot and Ankle Models

Over the past few decades, FE modeling of the foot and ankle complex has improved considerably; however, there is still room for improvement to fully utilize the benefits of this approach in medical and biomechanical research. New methods to create the 3D foot and ankle renditions that can reduce the time and effort to include muscles, tendons, and ligaments need to be developed. One way to approach this can be by making synergistic use of both CT and MRI scans during the 3D model generation procedure. Specifically, even though the CT scans can provide great details for bone structure, they are not capable of delivering the locations and orientations of muscles, tendons, and ligaments in the human foot. This is because soft tissue cells can be easily penetrated by X-ray, which results in low resolution on the CT-scan images. In contrast, MRI scans perform excellently in illustrating the soft tissue and muscle structures. Notably, due to the lower manufacturing cost and time, CT scans are generally more popular than MRI scans. CT scans are usually chosen as the reference source for developing the FE foot and ankle complex [42]. However, if one can stack the two types of images together, they can create a better, more hi-biofidelic foot and ankle 3D models with all the physiological details that combine all the benefits from MRI and CT scans. As a result, models developed using this new approach can have better anatomical representations of the foot and ankle components as well as greatly impact the simulation results' clinical relevance. Further, if the proper imaging of the geometries is not possible to capture using these two types of scans, especially in case of using prosthesis or implant devices, then 3D image processing software can be a useful source to create the 3D volume surfaces for each anatomical component. Some of the notable 3D image processing software and coding methods are GMSH [79], AUTODESK MESHMIXER (Autodesk, Inc., San Rafael, CA), MESHLAB [80], and NEKTAR++ [81].

Additionally, to improve the confidence of the simulation results, sound model calibration, verification, and validation methods need to be implemented. The calibration process is twofold and occurs prior to the verification and validation steps if sufficient experimental data are available. The first procedure is the materials (constitutive) model calibration using experimental mechanical response data. Then, one-element FE modeling is used to verify if the material constants chosen through the calibration process do produce a similar mechanical response as in the experimental data. Depending on the type of boundary value problem that is being simulated, appropriate strain rate, stress state, and other mechanical behavior data for muscles, tendons, ligaments, adipose tissue, skin, and bones need to be selected. Meanwhile, the second calibration procedure is applied for the entire FE foot and ankle model itself to calibrate the FE model parameters such that the FE results produce similar foot and ankle system level as in a gait movement experiment. For example, in foot and ankle movement analysis, if the inversion dataset is used for model calibration, then the plantarflexion dataset can be used for validation. Moreover, as the number of meshed elements in the FE models increases, a mesh convergence (verification) study should be implemented to ensure that the FE results converge as the mesh number increase. Additionally, the interfacial properties of different components in the foot and ankle model must also be carefully assessed to get the upper and lower bounds (margin-of-error bands) of the FE results. These interfacial properties include the interactions between bone versus (versus) bone, bone versus muscle, muscle versus tendon, and muscle versus soft tissue. Hence, the need for an advanced approach in collecting interfacial properties is crucial as obtaining the experimentally measured values of these properties between various components of the foot and ankle complex can be challenging. Notably, an alternative way to access the impact of the interfacial properties on the FE results would be to conduct one set of FE simulations with fully fixed interfacial properties and then conduct another set of FE simulation with slip interfacial properties. These two sets of FE results would also form the upper and lower bounds, within which any FE results that use realistic interfacial properties will fluctuate. After the verification and validation procedures are completed, the FE models are ready to simulate diverse boundary value problems of the foot and ankle complex movement within the strain rate range for which the material models were calibrated.

Finally, building a generalized foot and ankle model that is suitable for everyone is not feasible with the current procedure. To be more specific, the current approach only allows developing the FE foot and ankle complex for a particular individual, with no means to generalize and apply it to other patients. Consequently, since there are different anthropometries (e.g., foot sizes and types), a novel transformation method that can adjust and transform a reference foot model into a specific foot geometry needs to be developed. This transformation method can be done by creating a systematic approach to parameterize the characteristics of the foot, then utilizing novel transformation functions such as scaling factors—which based on the experimental and virtual motion capture markers on foot [82]—to modify and convert a prebuilt normal FE foot and ankle model into the particular model that is suitable for use in each specific study. The above-mentioned transformation process would be time-saving compared to the process of recreating the 3D volume surface of the foot and ankle using CT scans and MRI images. In theory, this novel

transformation method could reduce the time and resources required for FE foot model development as well as conserve the consistency among different studies.

Conclusions

The use of 3D computational FE models for the simulation of foot and ankle complex in recent studies has started to emerge as an adjuvant method to analyze the biomechanics of the foot, evaluate the performance of prosthesis devices, and predict the risk of injury during daily activities. The efficiency of the foot and ankle FE model has been demonstrated in various research studies as well as clinical studies. The purpose of this review was to discuss the details of the procedures to develop an accurate, biofidelic foot and ankle model, then provide the necessary information to calibrate, verify, and validate the said model as well as introduce the crucial steps and parameters in generating the simulation environment. In addition, the current applications of the FE foot and ankle model in various fields have also been reviewed. Furthermore, potential developments for those applications and FE approaches in foot–ankle models were discussed. To effectively enhance the simulation results, some of the possible improvements were also explained in this review, aiming to shorten the development time, increase the robustness of the model as well as propose a novel approach to accurately transform a specific foot structure from a reference foot and ankle complex model. Overall, further developments are required in the field of computational modeling and FEA to provide greater insights into the foot and ankle complex injury biomechanics.

Acknowledgment

This material is based upon work supported by the Department of Agricultural and Biological Engineering and the Center for Advanced Vehicular Systems at Mississippi State University.

P.P. wrote the paper, especially on model development procedure, literature review, and provided summary data for Appendix. R.P. and A.V. constructed the outline and drafted the abstract, history, and introduction section while A.B. wrote the discussion of model validation and verification. R.B., H.C., and A.K. provided great insight into human kinesiology and biomechanics of the foot and ankle anatomy as well as its corresponding discussion section. B.S. and J.B. aided in editing the paper and suggested suitable modifications. R.P. contributed to the discussion of FE applications and future development as well as the conclusion section. All authors reviewed the final paper.

Funding Data

- National Science Foundation (NSF) Division of Industrial Innovation and Partnerships (IIP) (No. NSF 18-511)—Partnerships for Innovation Award No. 1827652 (Funder ID: 10.13039/100000001).

Conflict of Interest

No potential conflict of interest was reported by the authors.

Appendix

Foot and Ankle Complex—Anatomy and Function. There are four movements of the foot and ankle complex: dorsiflexion, plantarflexion, inversion, and eversion, all of which are mainly controlled by eleven groups of muscle surrounding the ankle. Figure 5 illustrates the names and locations for each of these muscle groups. Additionally, Table 1 presents the relationships between these muscle groups and the corresponding foot and ankle movements. Through Fig. 5 and Table 1, the structure–function information can be conveyed more effectively, which aids readers in understanding the anatomy and function of these muscle groups and their influences on specific movements of the human foot and ankle complex.

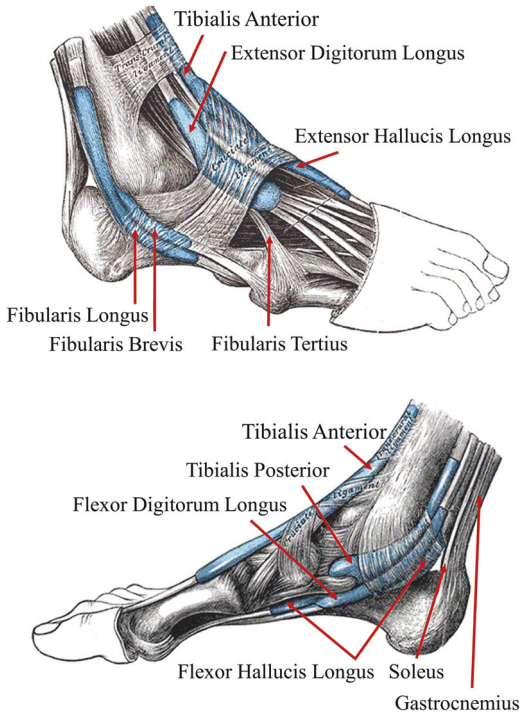

Fig. 5 Illustration of the foot and ankle complex muscle groups for Table 1 (modified from Fig. 1241 and 1242 of Gray's Anatomy—Public Domain [83])

Table 1 Muscle groups and their corresponding function in four basis foot and ankle movements

Muscle group	Function
Tibialis anterior	Dorsiflexion + inversion
Extensor hallucis longus	Dorsiflexion + inversion
Extensor digitorum longus	Dorsiflexion + eversion
Tibialis posterior	Plantarflexion + inversion
Flexor digitorum longus	Plantarflexion + inversion
Flexor hallucis longus	Plantarflexion + inversion
Gastrocnemius	Plantarflexion
Soleus	Plantarflexion
Fibularis longus	Eversion + plantarflexion
Fibularis brevis	Eversion + plantarflexion
Fibularis tertius	Dorsiflexion + eversion

A Brief History of Finite Element Modeling for Foot and Ankle Complex. Table 2 demonstrates the survey of notable studies utilizing FE models of foot ankle complex in diverse applications. The study's objectives are summarized along with the FE model characteristics and material properties are also reported. Additionally, the studies mentioned in this survey were also classified into four particular applications: foot and ankle model development, foot and ankle biomechanics analysis, models for foot disorders and injury predictions, and implants' and prostheses' performance assessment. Furthermore, each study's strengths

Table 2 A list of notable studies that use FE modeling for analyzing the foot and ankle complex biomechanics

Study and methods	FE model elements	Components	Material properties	Applications	Strength	Limitation
Foot and ankle model development						
Tannous et al. [27] — explicit	17,503 elements.	28 bones, 7 ankle ligaments, 3 retinacula, 3 layers of plantar soft tissues, and the Achilles tendon.	Linear elastic (bone, tendon, soft tissue), viscoelastic (ligament).	Develop the three-dimensional FE model of the human ankle/foot complex, which is a first step leading toward ankle injury criterion.	One of the first foot and ankle model that was developed and subjected to preliminary verifications against a limited set of data.	Missing material stress–strain curve for various components, lack of foot joints, articular surfaces and muscles.
Vijayaragavan et al. [29] — implicit	Not included.	26 bones, deltoid ligament, plantar fascia and Achilles tendons.	Linear elastic (all materials).	Develop a 3D anatomically realistic model of the ankle joint and the foot.	Implemented with various loading conditions to simulate stress distribution during different phases of gait.	Lack of validation with experimental data.
Ou et al. [61] — implicit	40,000 elements.	30 bones, soft tissue, plantar aponeurosis, ligaments and skin.	Linear elastic (bone, ligament), shell element (skin), hyperelastic Neo-Hookean models (soft tissue and plantar aponeurosis).	Evaluate the effect of skin during deformation of FE model by changing the elastic modulus of the skin and repeating the simulation.	Investigate the effect of skin on simulation results through a material sensitivity analysis. Results were validated by the displacements, stiffness and strain of foot components.	Different scenarios should be added to the simulation beside balanced standing. Soft tissue needed to be modeled with region-specific properties instead of homogeneous material.
Foot and ankle biomechanics analysis						
Cheung et al. [58] — static implicit	Not included.	28 bones, 72 ligaments, plantar fascia, cartilages and soft tissue.	Linear elastic (bone and cartilage), hyperelastic (soft tissue), truss element (ligament and plantar fascia).	Utilize a 3D FE model of the human foot and ankle to analyze the loading response of the plantar fascia in the standing foot with different magnitudes of Achilles tendon loading.	Cadaveric data of Achilles tendon was used to validate model results.	Linear elastic material properties were used for ligaments and bones, no surface interaction between bones, muscles and ligaments.
Quenneville et al. [65] — dynamic explicit	320,120 hexahedral elements.	Tibia and rigid parts.	Linear elastic (all materials).	Develop a FE model of the tibia using CT scans of a cadaveric foot to assess the response of tibia to short-duration, high-force axial loading.	The response to axial impact loading was thoroughly evaluated and compared to laboratory-based experimental results using cadaveric bone.	Difficulty in representing bone fracture, and its effect on geometry and energy absorption.
Qian et al. [38] — implicit quasi-static	4259 quadrilateral elements.	2D planar model: bones, phalanges and soft tissue.	Linear elastic (with damp coefficient for soft tissue).	Utilize 2D sagittal FE model of the foot to simulate gait cycle using data from motion capture.	Minimize computational cost through the use of 2D FE model. Utilize motion capture system to conduct simulation of foot during gait.	The simplification of the complex 3D foot model into 2D planar model led to some discrepancies in dynamic structural responses, resulting in a phase shift in peak pressure and delay in the plantar pressure response.

Table 2 (continued)

Study and methods	FE model elements	Components	Material properties	Applications	Strength	Limitation
Morales-Orcajo et al. [13] — quasi-static implicit	806,475 tetrahedral elements.	30 cortical bone, 18 trabecular bone, 22 cartilage, 29 tendons and muscle, 2 fascia segments and the soft tissue.	Linear elastic (bone, cartilage, muscle), Ogden (tendon), hyperelastic (fat tissue).	Analysis of the lower limb tendon forces effect on foot and ankle complex.	Nonlinear behavior of tendons was developed and their impacts were validated. Providing useful tools for clinical assessment.	Missing ligaments and lack of bone-to-bone contact. Overlapping muscle and tension components. Unable to measure muscle forces.
Filardi et al. [19] — static implicit	167,142 elements.	17 bones, skin, rigid wall and ligaments.	Linear elastic (bone and wall), truss connector (ligament), hyperelastic (soft tissue).	Develop a 3D FE model of the foot using MRI scans to analyze the effect of soft tissue stiffness on the plantar pressure distributions as well as internal load transfer.	Able to illustrate the effect of soft tissue stiffness on stress distributions of the foot in a bony and soft tissue structure.	Lack the incorporation of nonlinear and viscoelastic material properties for the ligamentous and soft tissue structures. Detailed muscular loading also needed.
Foot disorders and injury predictions						
Chen et al. [59] — static implicit	245,782 tetrahedral elements.	Bones, cartilages, ligaments, plantar fascia and soft tissue.	Linear elastic (bone and cartilage), hyperelastic (soft tissue), truss element (ligament and plantar fascia).	Develop a 3D FE model of human foot complex to predict the internal plantar soft-tissue deformation and stress.	Including soft tissue together with bones. Relative articulating movements of the bony joints were allowed in the entire foot.	Only standing loads were performed. Various loads specific to different phases of gait needed to be analyzed.
Sun et al. [62] — implicit	38,870 elements.	Bones, ligaments, plantar fascia and skin.	Linear elastic (bone, skin), tension-only elements (ligament, plantar fascia).	Investigate the effect of different foot arch height and evaluate the stress distribution on each foot arch type.	Able to modify model to create different arch heights and lengths using user-defined indices.	Lack of hyperelasticity and viscoelasticity characteristics implementation to mimic soft tissue.
Filardi et al. [40] — static implicit	50,999 tetrahedral elements.	Pelvis, femur, patella, fibula, tibia, foot and ligaments.	Nonlinear elastic (all materials).	Investigate the effect of stress shielding on the integrity and resistance of bone using FE model of human leg.	Results reveal interesting consequences deriving by taking into account the complete bony chain from pelvis to toes.	Viscoelastic properties of ligaments meniscus and cartilages were not considered. Predefined loading and boundary conditions needed to be further studied and refined.
Morales-Orcajo et al. [57] — quasi-static Implicit	783,000 tetrahedral elements.	28 bones, cartilages, 9 ligaments and 9 muscles.	Linear elastic (bones and cartilage), truss element (ligament), beam element (muscles).	Build a FE skeletal model of the foot to assess the development of Hallux Abducto Valgus (HAV) forefoot deformity.	Able to create abnormal FE foot model using CT scans of subject that included ligaments and cartilages by proposing a new skeletal parameter related to HAV.	Fat surrounding the skeletal was not simulated. Results were only applicable to hard tissue as it was simulated in a very simplified manner. Results cannot be compared directly with experimental measures at the time.

Table 2 (continued)

Study and methods	FE model elements	Components	Material properties	Applications	Strength	Limitation
Wong et al. [78] — implicit	Not included.	30 bones, soft tissue, muscle, skin and ligaments.	Linear elastic (bone), truss element (ligament and muscle), hyperelastic (skin and soft tissue).	Investigate the influence of impact velocity on the stress of calcaneus and talus as well as the risk of fracture using FE model.	Able to suggest the injury pattern and fracture mode of high energy trauma, providing insights in injury prevention and fracture management.	Trabecular and cortical bones were not segmented in midfoot and forefoot. The analysis of cortical bone was not conducted.
Smolen et al. [20] — explicit	450,580 hexahedral and 3954 shell elements.	26 bones, 67 ligaments and plantar soft tissue.	Linear elastic (bone), hyperelastic-Ogden rubber model (soft tissue), elastic force–strain response function (ligament).	Identify injury risk based on postures using foot and ankle complex model.	Success in determine the fracture thresholds and locations for each posture.	Locations of the strain gauges used in validation, the lack of soft tissue, and the number of tested specimens.
Gozar et al. [35] — static explicit	75,000 nodes.	26 bones and numerous connectors as ligaments and tendons.	Linear elastic (bone), beam connector (ligament), axial connector (tendon).	Analyze the biomechanics of the congenital clubfoot.	Utilize FE model to study the foot biomechanics of orthopedic patients, providing great advantages in both clinical and experimental circumstances.	Lack of various structural parameters and experimental data for a specific foot disorder (ex: clubfoot).
Implants and prostheses assessment						
Sopher et al. [36] — static implicit	53,000–77,000 elements.	Tibia, talar and 6 implant devices.	Linear elastic (bone and implant).	Use FE model to build and test the micromotion of TAR prosthesis under different conditions by applying force on the interested site of fixation.	Integrate FE model of tibia/talus and geometrical computer-aided-design models to test the behavior of the implants in various conditions.	Obtained results were not directly validated experimentally. Assumption of perfect contact between bone and the implant (not necessary in reality).
Wang et al. [30] — implicit	Not included.	28 bones, 103 ligaments, plantar fascia, nine groups of extrinsic muscles, a bulk of encapsulated soft tissue. Tibia/talar and mobile bearing implants.	Linear elastic (bone and implant), axial connector (muscle), tension-only truss element (ligament).	Compare the mechanical performance of foot/ankle complex with TAA and an intact one using FE model.	Successfully study the performance of an ankle prosthesis by incorporating motion analysis data.	Separation of cortical and trabecular components was needed. Lack of suitable boundary and loading conditions for TAA foots.

and limitations are also reported and discussed, all of which helps the reader in understanding the evolution of the foot and ankle complex's FE meshing and modeling procedures over time.

References

[1] Gribble, P. A., and Delahunt, E., 2019, "The International Ankle Consortium: Promoting Long-Term Stability in Ankle-Sprain Research," J. Athletic Train., **54**(6), pp. 570–571.

[2] Hertel, J., and Corbett, R. O., 2019, "An Updated Model of Chronic Ankle Instability," J. Athletic Train., **54**(6), pp. 572–588.

[3] Herzog, M. M., Kerr, Z. Y., Marshall, S. W., and Wikstrom, E. A., 2019, "Epidemiology of Ankle Sprains and Chronic Ankle Instability," J. Athletic Train., **54**(6), pp. 603–610.

[4] Kaminski, T. W., Needle, A. R., and Delahunt, E., 2019, "Prevention of Lateral Ankle Sprains," J. Athletic Train., **54**(6), pp. 650–661.

[5] Delahunt, E., and Remus, A., 2019, "Risk Factors for Lateral Ankle Sprains and Chronic Ankle Instability," J. Athletic Train., **54**(6), pp. 611–616.

[6] Kraemer, W., Denegar, C., and Flanagan, S., 2009, "Recovery From Injury in Sport: Considerations in the Transition From Medical Care to Performance Care," Sports Health, **1**(5), pp. 392–395.

[7] Demontiero, O., Vidal, C., and Duque, G., 2012, "Aging and Bone Loss: New Insights for the Clinician," Ther. Adv. Musculoskeletal Dis., **4**(2), pp. 61–76.

[8] Engelke, K., van Rietbergen, B., and Zysset, P., 2016, "FEA to Measure Bone Strength: A Review," Clin. Rev. Bone Miner. Metab., **14**(1), pp. 26–37.

[9] Ratchev, S., Liu, S., Huang, W., and Becker, A. A., 2006, "An Advanced FEA Based Force Induced Error Compensation Strategy in Milling," Int. J. Mach. Tools Manuf., **46**(5), pp. 542–551.

[10] Erdemir, A., Guess, T. M., Halloran, J., Tadepalli, S. C., and Morrison, T. M., 2012, "Considerations for Reporting Finite Element Analysis Studies in Biomechanics," J. Biomech., **45**(4), pp. 625–633.

[11] Chan, C. C., and Chau, K. T., 1991, "Design of Electrical Machines by the Finite Element Method Using Distributed Computing," Comput. Ind., **17**(4), pp. 367–374.

[12] Gupta, C., Marwaha, S., and Manna, M. S., 2009, "Finite Element Method as an Aid to Machine Design: A Computational Tool," COMSOL Conference Bangalore, COMSOL, Bangalore, India, Oct. 8–10.

[13] Morales-Orcajo, E., Souza, T. R., Bayod, J., and Barbosa de Las Casas, E., 2017, "Non-Linear Finite Element Model to Assess the Effect of Tendon Forces on the Foot-Ankle Complex," Med. Eng. Phys., **49**, pp. 71–78.

[14] Logan, D. L., 2007, *A First Course in the Finite Element Method*, 4th ed., Thomson Learning, Singapore.

[15] Abdel-Nasser, Y. A., 2013, "Frontal Crash Simulation of Vehicles Against Lighting Columns Using FEM," Alexandria Eng. J., **52**(3), pp. 295–299.

[16] Yamaguchi, S., Yamanishi, Y., Machado, L. S., Matsumoto, S., Tovar, N., Coelho, P. G., Thompson, V. P., and Imazato, S., 2018, "In Vitro Fatigue Tests and in Silico Finite Element Analysis of Dental Implants With Different Fixture/Abutment Joint Types Using Computer-Aided Design Models," J. Prosthodontics Res., **62**(1), pp. 24–30.

[17] Horstemeyer, M. F., 2012, *Integrated Computational Materials Engineering (ICME) for Metals: Using Multiscale Modeling to Invigorate Engineering Design With Science*, Wiley, Hoboken, NJ.

[18] Jain, M. L., Govind Dhande, S., and Vyas, N. S., 2011, "Virtual Modeling of an Ankle Foot Orthosis for Correction of Foot Abnormality," Rob. Comput. Integr. Manuf., **27**(2), pp. 257–260.

[19] Filardi, V., 2018, "Finite Element Analysis of the Foot: Stress and Displacement Shielding," J. Orthop., **15**(4), pp. 974–979.

[20] Smolen, C., and Quenneville, C. E., 2017, "A Finite Element Model of the Foot/Ankle to Evaluate Injury Risk in Various Postures," Ann. Biomed. Eng., **45**(8), pp. 1993–2008.

[21] Murni, N. S., Dambatta, M. S., Yeap, S. K., Froemming, G. R. A., and Hermawan, H., 2015, "Cytotoxicity Evaluation of Biodegradable Zn-3 Mg Alloy Toward Normal Human Osteoblast Cells," Mater. Sci. Eng. C, **49**, pp. 560–566.

[22] Sahu, N. K., and Kaviti, A. K., 2016, "A Review of Use FEM Techniques in Modeling of Human Knee Joint," J. Biomimetics, Biomater. Biomed. Eng., **28**, pp. 14–25.

[23] Cooper, R. J., Wilcox, R. K., and Jones, A. C., 2019, "Finite Element Models of the Tibiofemoral Joint: A Review of Validation Approaches and Modelling Challenges," Med. Eng. Phys., **74**, pp. 1–12.

[24] Parashar, S. K., and Sharma, J. K., 2016, "A Review on Application of Finite Element Modelling in Bone Biomechanics," Perspect. Sci., **8**, pp. 696–698.

[25] Behforootan, S., Chatzistergos, P., Naemi, R., and Chockalingam, N., 2017, "Finite Element Modelling of the Foot for Clinical Application: A Systematic Review," Med. Eng. Phys., **39**, pp. 1–11.

[26] Rodgers, M. M., 1988, "Dynamic Biomechanics of the Normal Foot and Ankle During Walking and Running," Phys. Ther., **68**(12), pp. 1822–1830.

[27] Tannous, R. E., Bandak, F. A., Toridis, T. G., and Eppinger, R. H., 1996, "Three-Dimensional Finite Element Model of the Human Ankle: Development and Preliminary Application to Axial Impulsive Loading," Stapp Car Crash Conference Proceedings, Warrendale, PA, Nov. 4–6, pp. 219–236.

[28] Windrich, M., Grimmer, M., Christ, O., Rinderknecht, S., and Beckerle, P., 2016, "Active Lower Limb Prosthetics: A Systematic Review of Design Issues and Solutions," Biomed. Eng. Online, **15**(Suppl. 3), p. 140.

[29] Vijayaragavan, E., and Gopal, T. V., 2016, "Biomechanical Modeling of Human Foot Using Finite Element Methods," Indian J. Sci. Technol., **9**(31), pp. 1–5.

[30] Wang, Y., Li, Z., Wong, D. W.-C. C., Cheng, C.-K. K., and Zhang, M., 2018, "Finite Element Analysis of Biomechanical Effects of Total Ankle Arthroplasty on the Foot," J. Orthop. Transl., **12**, pp. 55–65.

[31] Pehde, C. E., Bennett, J., Lee Peck, B., and Gull, L., 2020, "Development of a 3-D Printing Laboratory for Foot and Ankle Applications," Clin. Podiatric Med. Surg., **37**(2), pp. 195–213.

[32] Dal Maso, A., and Cosmi, F., 2018, "3D-Printed Ankle-Foot Orthosis: A Design Method," 35th DANUBIA Adria Symposium on Advances in Experimental Mechanics, Sinaia, Romania, Sept. 25–28, pp. 127–128.

[33] Milusheva, S. M., Tosheva, E. Y., Hieu, L. C., Kouzmanov, L. V., Zlatov, N., and Toshev, Y. E., 2006, "Personalised Ankle-Foot Orthoses Design Based on Reverse Engineering," Intelligent Production Machines and Systems—Second I*PROMS Virtual International Conference, July 3–14, pp. 253–257.

[34] Filardi, V., and Milardi, D., 2017, "Experimental Strain Analysis on the Entire Bony Leg Compared With FE Analysis," J. Orthop., **14**(1), pp. 115–122.

[35] Gozar, H., Chira, A., Nagy, Ö., and Derzsi, Z., 2018, "Medical Use of Finite Element Modeling of the Ankle and Foot," J. Interdiscip. Med., **3**(1), pp. 34–38.

[36] Sopher, R. S., Amis, A. A., Calder, J. D., and Jeffers, J. R. T., 2017, "Total Ankle Replacement Design and Positioning Affect Implant-Bone Micromotion and Bone Strains," Med. Eng. Phys., **42**, pp. 80–90.

[37] Sadeghian, F., Zakerzadeh, M. R., Karimpour, M., and Baghani, M., 2019, "Numerical Study of Patient-Specific Ankle-Foot Orthoses for Drop Foot Patients Using Shape Memory Alloy," Med. Eng. Phys., **69**, pp. 123–133.

[38] Qian, Z., Ren, L., Ding, Y., Hutchinson, J. R., and Ren, L., 2013, "A Dynamic Finite Element Analysis of Human Foot Complex in the Sagittal Plane During Level Walking," PLoS One, **8**(11), p. e79424.

[39] Cheung, J. T. M., Zhang, M., Leung, A. K. L., and Fan, Y. B., 2005, "Three-Dimensional Finite Element Analysis of the Foot During Standing—A Material Sensitivity Study," J. Biomech., **38**(5), pp. 1045–1054.

[40] Filardi, V., 2014, "FE Analysis of Stress and Displacements Occurring in the Bony Chain of Leg," J. Orthop., **11**(4), pp. 157–165.

[41] Shin, J., Yue, N., and Untaroiu, C. D., 2012, "A Finite Element Model of the Foot and Ankle for Automotive Impact Applications," Ann. Biomed. Eng., **40**(12), pp. 2519–2531.

[42] Smith-Bindman, R., Miglioretti, D. L., and Larson, E. B., 2008, "Rising Use of Diagnostic Medical Imaging in a Large Integrated Health System," Health Aff., **27**(6), pp. 1491–1502.

[43] Rajapakse, C. S., Kobe, E. A., Batzdorf, A. S., Hast, M. W., and Wehrli, F. W., 2018, "Accuracy of MRI-Based Finite Element Assessment of Distal Tibia Compared to Mechanical Testing," Bone, **108**, pp. 71–78.

[44] Kraeima, J., Dorgelo, B., Gulbitti, H. A., Steenbakkers, R. J. H. M., Schepman, K. P., Roodenburg, J. L. N., Spijkervet, F. K. L., Schepers, R. H., and Witjes, M. J. H., 2018, "Multi-Modality 3D Mandibular Resection Planning in Head and Neck Cancer Using CT and MRI Data Fusion: A Clinical Series," Oral Oncol., **81**, pp. 22–28.

[45] Patrick, S., Birur, N., Gurushanth, K., Raghavan, A., and Gurudath, S., 2017, "Comparison of Gray Values of Cone-Beam Computed Tomography With Hounsfield Units of Multislice Computed Tomography: An In Vitro Study," Indian J. Dent. Res., **28**(1), p. 66.

[46] Floyd, R., and Thompson, C. W., 2018, *Manual of Structural Kinesiology*, McGraw-Hill, New York.

[47] Brockett, C. L., and Chapman, G. J., 2016, "Biomechanics of the Ankle," Orthop. Trauma, **30**(3), pp. 232–238.

[48] Floyd, R. T., 2015, "Basic Biomechanical Factors and Concepts," *Manual of Structural Kinesiology*, McGraw-Hill Education, New York, pp. 69–89.

[49] Buzug, T. M., 2008, *Computed Tomography: From Photon Statistics to Modern Cone-Beam CT*, Springer, Manhattan, NY.

[50] Heymsfield, S. B., Lohman, T., Wang, Z., and Going, S. B., 2005, *Human Body Composition*, Human Kinetics, Champaign, IL.

[51] Prokop, M., 2003, *Spiral and Multislice Computed Tomography of the Body*, Thieme, Stuttgart, Germany.

[52] Sysnopsys, Inc., 2017, "Simpleware Software Reference Guide," Sysnopsys, Mountain View, CA.

[53] Burkhart, T. A., Andrews, D. M., and Dunning, C. E., 2013, "Finite Element Modeling Mesh Quality, Energy Balance and Validation Methods: A Review With Recommendations Associated With the Modeling of Bone Tissue," J. Biomech., **46**(9), pp. 1477–1488.

[54] Gray, H., 2009, *Gray's Anatomy: With Original Illustrations by Henry Carter*, Arcturus Publishing, London.

[55] Golanó, P., Vega, J., de Leeuw, P. A. J., Malagelada, F., Manzanares, M. C., Götzens, V., and van Dijk, C. N., 2010, "Anatomy of the Ankle Ligaments: A Pictorial Essay," Knee Surg., Sports Traumatol. Arthroscopy, **18**(5), pp. 557–569.

[56] Netter, F. H., 2018, *Netter Atlas of Human Anatomy*, 7th ed., Elsevier, New York.

[57] Morales-Orcajo, E., Bayod, J., Becerro-de-Bengoa-Vallejo, R., Losa-Iglesias, M., and Doblare, M., 2015, "Influence of First Proximal Phalanx Geometry on Hallux Valgus Deformity: A Finite Element Analysis," Med. Biol. Eng. Comput., **53**(7), pp. 645–653.

[58] Cheung, J. T. M., Zhang, M., and An, K. N., 2006, "Effect of Achilles Tendon Loading on Plantar Fascia Tension in the Standing Foot," Clin. Biomech., **21**(2), pp. 194–203.

[59] Chen, W. M., Lee, T., Lee, P. V. S., Lee, J. W., and Lee, S. J., 2010, "Effects of Internal Stress Concentrations in Plantar Soft-Tissue-a Preliminary Three-Dimensional Finite Element Analysis," Med. Eng. Phys., **32**(4), pp. 324–331.
[60] Mkandawire, C., Ledoux, W., Sangeorzan, B., and Ching, R., 2001, "Hierarchical Cluster Analysis of Area and Length of Foot and Ankle Ligaments," Proceedings of the 25th Annual Meeting of the American Society of Biomechanics, San Diego, CA, Aug. 8–11, pp. 8–11.
[61] Ou, H., Qaiser, Z., Kang, L., and Johnson, S., 2018, "Effect of Skin on Finite Element Modeling of Foot and Ankle During Balanced Standing," J. Shanghai Jiaotong Univ., **23**(1), pp. 132–137.
[62] Sun, P. C., Shih, S. L., Chen, Y. L., Hsu, Y. C., Yang, R. C., and Chen, C. S., 2012, "Biomechanical Analysis of Foot With Different Foot Arch Heights: A Finite Element Analysis," Comput. Methods Biomech. Biomed. Eng., **15**(6), pp. 563–569.
[63] Fellipa, C., 2012, *FEM Modeling: Mesh, Loads and BCs*, University of Colorado, Boulder, CO, Chap. 7.
[64] Knupp, P., 2007, "Remarks on Mesh Quality (No. SAND2007-8128C)," Sandia National Laboratories (SNL-NM), Albuquerque, NM.
[65] Quenneville, C. E., and Dunning, C. E., 2011, "Development of a Finite Element Model of the Tibia for Short-Duration High-Force Axial Impact Loading," Comput. Methods Biomech. Biomed. Eng., **14**(2), pp. 205–212.
[66] Ray, M. H., Mongiardini, M., Atahan, A. O., Plaxico, C., and Anghileri, M., 2008, "Recommended Procedures for Verification and Validation of Computer Simulations Used for Roadside Safety Applications," National Cooperative Highway Research Program (NCHRP) Project, pp. 22–24.
[67] Cheng, Z. Q., Thacker, J. G., Pilkey, W. D., Hollowell, W. T., Reagan, S. W., and Sieveka, E. M., 2001, "Experiences in Reverse-Engineering of a Finite Element Automobile Crash Model," Finite Elem. Anal. Des., **37**(11), pp. 843–860.
[68] Zhang, Z., Zhang, W., Zhai, Z. J., and Chen, Q. Y., 2007, "Evaluation of Various Turbulence Models in Predicting Airflow and Turbulence in Enclosed Environments by CFD—Part 2: Comparison With Experimental Data From Literature," HVAC R Res., **13**(6), pp. 871–886.
[69] Moore, S. M., Ellis, B., Weiss, J. A., McMahon, P. J., and Debski, R. E., 2010, "The Glenohumeral Capsule Should Be Evaluated as a Sheet of Fibrous Tissue: A Validated Finite Element Model," Ann. Biomed. Eng., **38**(1), pp. 66–76.
[70] Torcasio, A., Zhang, X., Duyck, J., and Van Lenthe, G. H., 2012, "3D Characterization of Bone Strains in the Rat Tibia Loading Model," Biomech. Model. Mechanobiol., **11**(3–4), pp. 403–410.
[71] Schober, P., Boer, C., and Schwarte, L. A., 2018, "Correlation Coefficients: Appropriate Use and Interpretation," Anesth. Analg., **126**(5), pp. 1763–1768.
[72] Luczak, T., Saucier, D., Burch, R. F. V., Ball, J. E., Chander, H., Knight, A., Wei, P., and Iftekhar, T., 2018, "Closing theWearable Gap: Mobile Systems for Kinematic Signal Monitoring of the Foot and Ankle," Electronics, **7**(7), pp. 1–24.
[73] Chander, H., Stewart, E., Saucier, D., Nguyen, P., Luczak, T., Ball, J. E., Knight, A. C., Smith, B. K., V, R. F. B., and Prabhu, R. K., 2019, "Closing the Wearable Gap—Part III: Use of Stretch Sensors in Detecting Ankle Joint Kinematics During Unexpected and Expected Slip and Trip Perturbations," Electronics, **8**(10), p. 1083.
[74] Saucier, D., Luczak, T., Nguyen, P., Davarzani, S., Peranich, P., Ball, J. E., Burch, R. F., Smith, B. K., Chander, H., Knight, A., and Prabhu, R. K., 2019, "Closing the Wearable Gap—Part II: Sensor Orientation and Placement for Foot and Ankle Joint Kinematic Measurements," Sensors, **19**(16), p. 3509.
[75] Khalid, G. A., Prabhu, R. K., Arthurs, O., and Jones, M. D., 2019, "A Coupled Physical-Computational Methodology for the Investigation of Short Fall Related Infant Head Impact Injury," Forensic Sci. Int., **300**, pp. 170–186.
[76] Wang, H., and Brown, S. R., 2017, "The Effects of Total Ankle Replacement on Ankle Joint Mechanics During Walking," J. Sport Heal. Sci., **6**(3), pp. 340–345.
[77] Shahar, F. S., Hameed Sultan, M. T., Lee, S. H., Jawaid, M., Md Shah, A. U., Safri, S. N. A., and Sivasankaran, P. N., 2019, "A Review on the Orthotics and Prosthetics and the Potential of Kenaf Composites as Alternative Materials for Ankle-Foot Orthosis," J. Mech. Behav. Biomed. Mater., **99**, pp. 169–185.
[78] Wong, D. W. C., Niu, W., Wang, Y., and Zhang, M., 2016, "Finite Element Analysis of Foot and Ankle Impact Injury: Risk Evaluation of Calcaneus and Talus Fracture," PLoS One, **11**(4), p. e0154435.
[79] Geuzaine, C., and Remacle, J.-F., 2009, "Gmsh: A Three-Dimensional Finite Element Mesh Generator With Built-in Pre- and Post-Processing Facilities," Int. J. Numer. Methods Eng., **79**(11), pp. 1309–1331.
[80] Cignoni, P., Callieri, M., Corsini, M., Dellepiane, M., Ganovelli, F., and Ranzuglia, G., 2008, "MeshLab: An Open-Source Mesh Processing Tool," Sixth Eurographics Italian Chapter Conference, Salerno, Italy, July 2–4, pp. 129–136.
[81] Moxey, D., Cantwell, C. D., Bao, Y., Cassinelli, A., Castiglioni, G., Chun, S., Juda, E., Kazemi, E., Lackhove, K., Marcon, J., Mengaldo, G., Serson, D., Turner, M., Xu, H., Peiró, J., Kirby, R. M., and Sherwin, S. J., 2020, "Nektar++: Enhancing the Capability and Application of High-Fidelity Spectral/Hp Element Methods," Comput. Phys. Commun., **249**, p. 107110.
[82] Hicks, J., 2018, "How Scaling Works, OpenSim Documentation," accessed Apr. 20, 2020, https://simtk-confluence.stanford.edu:8443/display/OpenSim/How+Scaling+Works
[83] Gray, H., 1918, *Anatomy of the Human Body*, 20th ed., Lea and Febiger, Philadelphia, PA.